photonics

MDPI

Article

Experimental Evaluation of Impairments in Unrepeatered DP-16QAM Link with Distributed Raman Amplification

Xiaodan Pang [1,2], Oskars Ozolins [1], Atalla El-Taher [3,*], Richard Schatz [2], Gunnar Jacobsen [1], Sergey Sergeyev [3] and Sergei Popov [2]

1 Networking and Transmission Laboratory, Acreo Swedish ICT AB, Kista SE-16425, Sweden; xiaodan.pang@acreo.se (X.P.); oskars.ozolins@acreo.se (O.O.); gunnar.jacobsen@acreo.se (G.J.)
2 Optics and Photonics Division, Royal Institute of Technology (KTH), Kista SE-16440, Sweden; rschatz@kth.se (R.S.); sergeip@kth.se (S.P.)
3 Aston Institute of Photonic Technologies, Aston University, Birmingham B4 7ET, UK; s.sergeyev@aston.ac.uk
* Correspondence: eltaheae@aston.ac.uk; Tel.: +44-121-204-3524

Received: 13 January 2017; Accepted: 6 March 2017; Published: 8 March 2017

Abstract: The transmission impairments of a Raman amplified link using dual-polarization 16-quadrature amplitude modulation (DP-16QAM) are experimentally characterized. The impact of amplitude and phase noise on the signal due to relative intensity noise (RIN) transfer from the pump are compared for two pumping configurations: first-order backward pumping and bi-directional pumping. Experimental results indicate that with increased Raman backward pump power, though the optical signal-to-noise ratio (OSNR) is increased, so is the pump-induced amplitude and phase noise. The transmission performance is firstly improved by the enhanced OSNR at a low pump power until an optimum point is reached, and then the impairments due to pump-induced noise start to dominate. However, the introduction of a low pump power in the forward direction can further improve the system's performance.

Keywords: Raman amplification; coherent communications; fiber optics communications

1. Introduction

Unrepeatered transmission systems provide a low-complexity and cost-effective solution for point-to-point connections on the order of a few hundred kilometers. The main objective for these systems is to achieve a single-span system between the points of interest without any in-line active elements between the terminals. Recently, high-order modulation formats and coherent detection using digital signal processing (DSP) have been introduced to increase the transport capacity. In these systems, the distributed Raman fiber amplifier (DFRA) is an attractive alternative to the conventional lumped erbium-doped fiber amplifier (EDFA). The DRFA ensures a relatively constant power distribution of the optical signals along the link and thereby improves the optical signal-to-noise ratio (OSNR) and the fiber nonlinearity tolerance [1–7]. Using DRFA with a large effective area fiber, unrepeatered transmission of a 30 Gbaud dual-polarization quadrature phase shift keying (DP-QPSK) over 444 km [2] and a 28 Gbaud DP-16 quadrature amplitude modulation (DP-16QAM) over 240 km [3,4] have been demonstrated. Unrepeatered transmission of a 40 × 256 Gb/s DP-16QAM signal over an ultra-low loss fiber with a very large effective area was demonstrated by using a first-order backward-pumped DRFA combined with a discrete EDFA at the receiver [5]. Transmission performance analysis was performed for differential phase shift keying (DPSK) transmission using standard fiber and second-order Raman amplification in [6], showcasing the different balance between impairments for different transmission lengths and higher-order distributed amplification. Recently, an unrepeatered Nyquist PDM-16QAM transmission over 364 km was demonstrated using Raman amplification and multi-channel digital back-propagation [7].

In DRFAs, the intensity fluctuations of the pump will induce both intensity and phase noise of the received signal. This is known as relative intensity noise (RIN) transfer which deteriorates the system performance and limits the system reach. The effect of RIN transfer on the intensity noise of the received signal has been intensively investigated in intensity modulation direct-detection systems [8–10]. The results show that the characteristics of the RIN transferred to the signal are strongly affected by different aspects, for example fiber dispersion, pumping configuration, and polarization-dependent gain [11–15]. The RIN transfer to both the amplitude and phase noise of multilevel coherent optical communication systems using DRFA has been studied using numerical analysis and system simulations, and evaluated with both unrepeatered and repeatered transmission experiments [16–21]. The stochastic intensity fluctuations of the Raman pump laser induce extra phase noise of the signal due to the pump signal cross-phase modulation. This is known as relative phase noise (RPN) and it degrades the system performance of phase-sensitive detection schemes. For example, the analytical model for the statistical property of RPN in first- and higher-order distributed Raman amplifiers [15] indicates that the impairments dependent on the Raman pumping order and RIN tolerance are different for each configuration. The study also shows that for the multi-level modulation format, in addition to RIN and RPN, Raman pump RIN will also induce polarization crosstalk through the cross-polarization modulation effect which has about the same impact on the performance as the RPN. A comprehensive theoretical and simulation study of the RPN was presented for M-ary phase shift keying (PSK) and 16QAM modulation formats in Reference [18]. The RPN-induced impairment was evaluated and compared for QPSK, 8PSK, 16PSK, and 16QAM signals. We have previously experimentally characterized the pump noise–induced impairments of an unrepeatered single polarization of a 28 Gbaud 16QAM link using backward-pumped Raman amplification [22], and for a dual-polarization 28 Gbaud 16QAM link [23] using bidirectionally pumped Raman amplification.

In this paper we report on a systematic experimental characterization of both the amplitude and phase noise of the signal due to RIN transfer from the Raman pump and evaluate the transmission impairments of a coherent DP-16QAM link using first-order pumped Raman amplification in a standard single-mode fiber (SSMF). We adopt a frequency domain representation approach to reconstruct the noise enhancement due to the Raman pump RIN transfer in both amplitude and phase. Regarding the transmission, we first evaluate the maximum reach, determined by the 7%-overhead hard-decision forward error correction (HD-FEC) threshold, of a backward pumping scheme. We subsequently investigate the transmission improvement one can achieve with the aid of additional forward pumping. For each pumping scheme, the phase noise and amplitude noise are measured as a function of the Raman pump power. Three different carrier phase recovery (CPR) algorithms are tested and compared for each transmission scenario: decision-directed phase-lock-loop (DDPLL) [24], two-stage feed-forward based on QPSK partitioning (QPSKP) with a sliding window average [25] and feed-forward based on blind phase search (BPS) [26,27].

This paper is organized as follows. In Section 2, we present the experimental setup to evaluate DFRA-induced impairments. Then we show and discuss the obtained results in Section 3. The conclusions are finally drawn in Section 4.

2. Experimental Setup

The experimental setup for signal transmission and noise characterization is shown in Figure 1. For transmission, a pseudo-random bit sequence with word length of $2^{15} - 1$ and its negated pattern are generated by a pulse pattern generator (PPG) operating at 28 Gbaud. Decorrelation is performed by delaying the negated pattern by 84 bits. A two-bit digital to analog converter (DAC) with 19 GHz analog bandwidth is employed to convert the binary sequences into four-level pulse amplitude modulation signals, where an additional 77-symbol delay is introduced between the two outputs to drive an IQ modulator with 25 GHz 3 dB bandwidth to generate an optical

28 Gbaud 16QAM. The transmitter external cavity laser (ECL) at 1550 nm has a linewidth of ~40 kHz. Polarization multiplexing (PolMux) emulation is performed after the IQ modulator to achieve 224 Gbit/s DP-16QAM. An optical booster, an optical bandpass filter (OBPF) with bandwidth of 1.2 nm and a variable optical attenuator (VOA) are placed before the fiber link for OSNR adjustment.

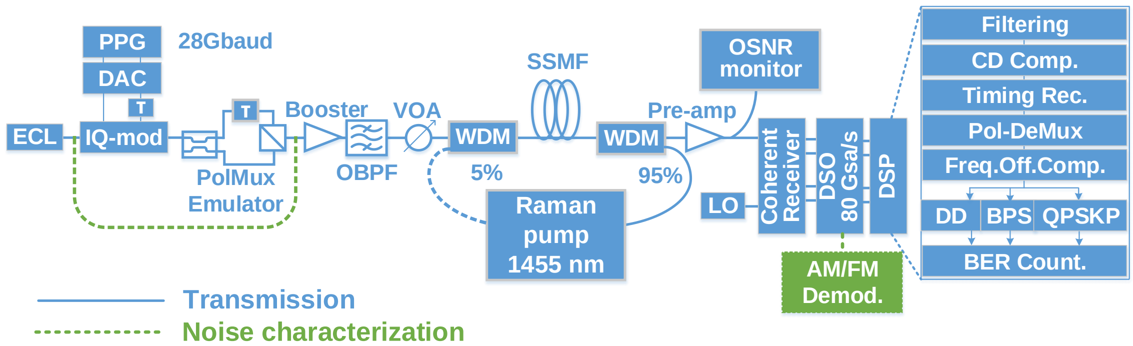

Figure 1. Experimental setup of distributed Raman amplified coherent transmission link. PPG: pulse pattern generator; DAC: digital-to-analog converter; WDM: wavelength division multiplexer; SSMF: standard single mode fiber; LO: local oscillator; DSO: digital storage oscilloscope; DDPLL: decision-directed phase-lock-loop; BPS: blind phase search; QPSKP: QPSK partitioning.

The transmission link is comprised of 200 km SSMF. First order pump at 1455 nm (PYL-1-1455-R, IPG Photonics, Oxford, MA, USA) is used to Raman amplify the signal which is divided into two parts 95% (backward) and 5% (forward) for distributed Raman amplification. An automatic gain controlled pre-amplifier EDFA with fixed output power is placed after the link. A coherent receiver with a ~40 kHz linewidth local oscillator (LO) and an 80 GSa/s digital storage oscilloscope (DSO) are used for detection. Signal demodulation is performed off-line with a DSP chain consisting of low pass filtering; chromatic dispersion (CD) compensation, timing recovery, polarization de-multiplexing and three different CPR methods before a bit-error-rate counter.

For a better understanding of the signal impairments induced by the distributed Raman amplification, we also characterized the amplitude and frequency noise of the received signal with the use of the digital coherent receiver based on the method described in [28]. In this measurement the transmitter laser is unmodulated and transmitted over the Raman amplified link with different pump configurations.

3. Results

The OSNR improvement using distributed Raman amplification was first evaluated. Figure 2 illustrates the measured OSNR versus the power of the first-order Raman pump for two pumping schemes, first using backward pumping with 95% of the pump power and second using bidirectional pumping, using the remaining 5% pump power for co-pumping. The experiments were done at two launched powers, 5 and 2 dBm, into the 200 km SSMF link. From Figure 2 it is observed that with 95% backward pumping, the received signal OSNR increased with the pump power compared to the reference case when the Raman pump was off. In addition, with the extra 5% of the power in the forward pumping, the OSNR enhancement was higher, especially at high power. It is important to note that the maximum forward pump used was only 40 mW.

In coherent optical communication systems using multi-level modulation formats, a high OSNR only is not enough to ensure a good transmission quality since other impairments such as the phase noise have a large impact on the system performance [18]. Therefore, we characterized the received signal amplitude and phase noise induced by the Raman pump RIN transfer.

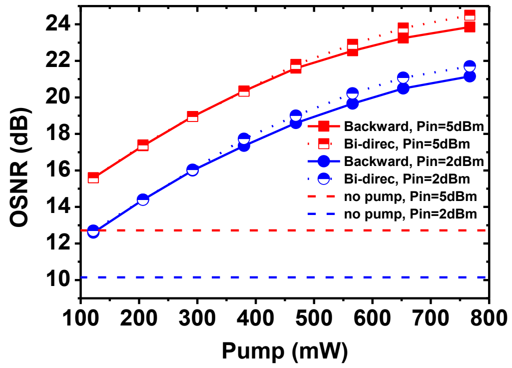

Figure 2. OSNR versus Raman pump power for two pumping schemes, backward pumping only with 95% and backward pumping with 95% together with co-pumping with 5% for two different launching powers.

Figure 3 shows the measured relative frequency noise and amplitude noise power spectrum density (PSD) of the received signal after bidirectional Raman amplification for different pump powers. All selected cases are with a 200 km SSMF length and a 5 dBm launched power. In this measurement, the transmitter laser was unmodulated and transmitted over the Raman amplified link with different pump configurations, as shown with the green dots in Figure 1. It is noted that this method characterizes the combined noise properties from both the received signal and the narrow linewidth LO. From the frequency noise PSD shown in Figure 3a, one can see that with a low Raman pump power, the noise shows a property that can be closely approximated as white phase noise. However, at a high pump power, the frequency noise level in the low frequency regime rises, while at the high frequency side the level decreases, which is due to the improvement of the signal OSNR (as shown in Figure 2). It is noted that there are spurs rising at around 11 GHz at the high pump power, which we attribute to the stimulated Brillouin scattering.

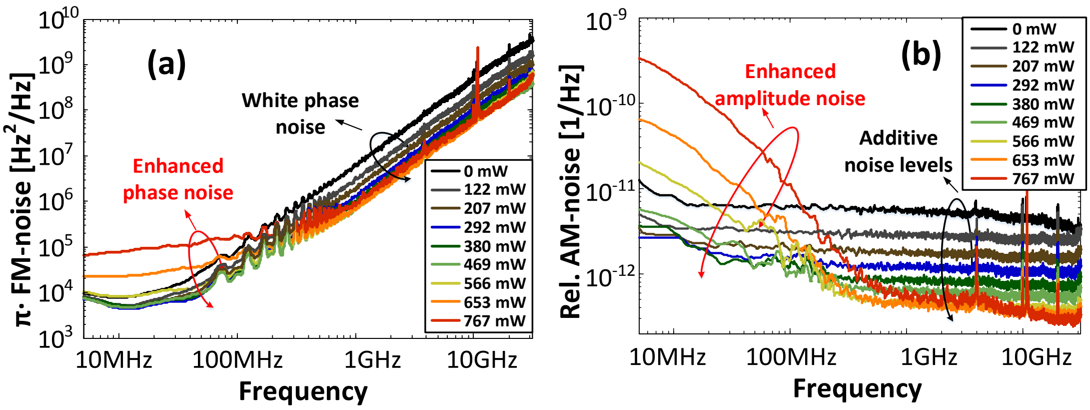

Figure 3. (**a**) Measured frequency noise and (**b**) relative amplitude noise power spectrum density for different pump powers. For all selected cases, the launched power = 5 dBm, fiber length = 200 km.

Similarly, from Figure 3b it is observed that as the pump power increases, the amplitude noise level at the high frequency side decreases, which is also due to the improvement of the signal OSNR. However, at the lower frequency regime a rise of the noise level at a higher pump power is observed. This noise enhancement can be attributed to the RIN transfer from the Raman pump. It is noted that the frequency regime of the enhanced noise is important for a potential effective mitigation by optical or digital means, as it defines the mitigation bandwidth of the optical or digital filter.

The Q factor (calculated from the measured bit error rate) is presented in Figure 4 as a function of the Raman pump power. The results for 200 km at a launched signal power of 5 and 2 dBm with the two different pumping schemes were taken after demodulation by the DDPLL, QPSKP and BPS algorithms, respectively. From the results it can be seen that with the increase of the pump power, the performance firstly improves due to the enhanced OSNR as shown in Figure 2. The optimum was found at around 550 mW in all cases. Figure 5 shows the constellations of DP-16QAM with the bidirectional pumping scheme for different pump powers. It is noted that in the constellations with a high pump power, nonlinear distortions are not clearly observed. The signal suffers from the induced amplitude and phase noise as shown in Figure 3, indicating that the induced noise dominates the performance despite the high OSNR values at the higher pump power. Consequently, unrepeatered coherent transmission should be optimized by balancing the signal OSNR and the Raman pump–induced impairments. By comparing the backward and bidirectional pumping schemes, we could observe a clear performance improvement around the optimum pump power, enabling the bidirectional pumping scheme to achieve a Q factor above the 8.5 dB HD-FEC limit after 200 km SSMF unrepeatered transmission. Moreover, it was observed that the BPS slightly outperformed DDPLL and QPSKP in mitigating the Raman-induced impairments, thanks to the accurate phase tracking capability at the high OSNR [27]. One should note that due to the experimental constraints, the power ratio between the forward and backward pump was fixed during this work; however, it is worth further investigation as an important aspect to draw a more generic conclusion. Additionally, a longer fiber span, higher modulation orders, as well as higher-order pumping schemes are to be investigated in our further studies.

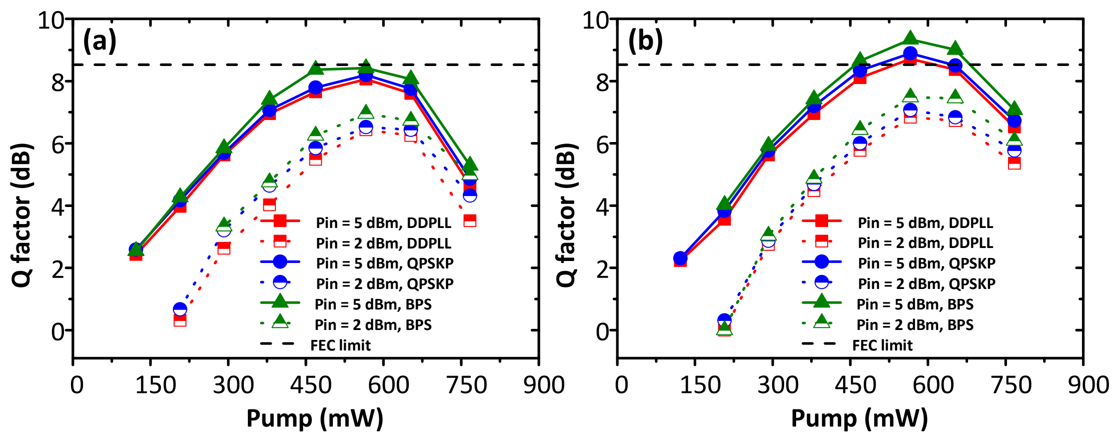

Figure 4. Q factor versus pump power for both (**a**) backward and (**b**) bidirectional pumping schemes with DDPLL, QPSKP and BPS algorithms, respectively, for launched signal powers of 5 and 2 dBm.

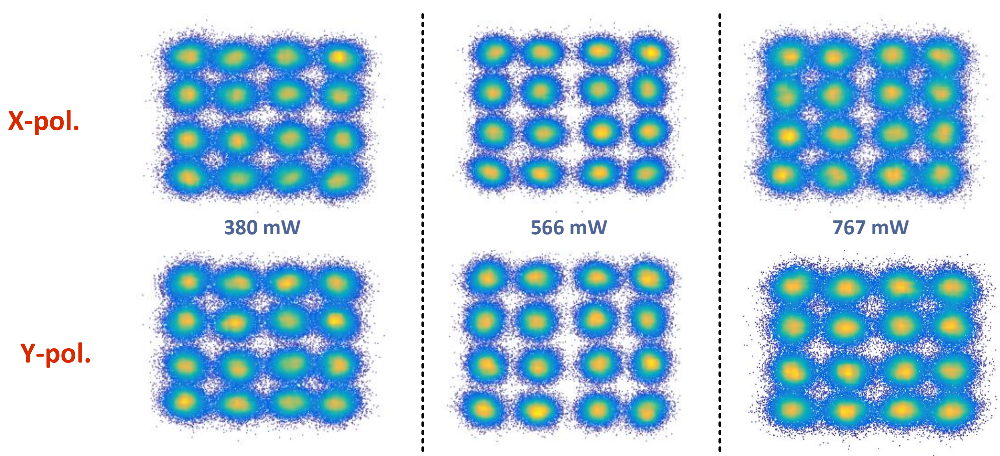

Figure 5. Constellations of DP-16QAM versus pump power for bidirectional pumping scheme for launched signal power of 5 dBm.

4. Conclusions

We have experimentally characterized the induced amplitude and phase noise due to the RIN of the Raman pump and studied their impact on the system performance of an unrepeatered 224 Gbit/s DP-16QAM link. The results show that a Q factor above the 8.5 dB HD-FEC limit after 200 km SSMF can be achieved with a bidirectional pumping scheme, using an optimized pump power and a small fraction (5%) of the pump in the forward direction. At low pump powers, additive noise due to a low OSNR is the dominant noise source, while at high pump powers, the induced noise from the Raman pump dominates. Additionally, the noise enhancement in both the amplitude and phase was observed to concentrate on the low-frequency regime, while the high-frequency regime was not as influenced. This indicates that the system performance may be further improved at high pump powers by suppressing the RIN transfer or by using advanced higher-order pumping schemes, or with certain digital mitigation methods focusing on low-frequency noise suppression. Further experimental studies for various types of impairments and their balance is required for the optimal design of the advanced multi-level modulation format signal–based unrepeatered transmission systems using higher-order DRFA. On the other hand, RPN impairment mitigation with more powerful DSP algorithms is worth investigating.

Acknowledgments: This work was supported by EU projects ICONE, gr. # 608099, GRIFFON, gr. # 324391 and Vetenskapsrädet PHASE, gr. #2016-04510. The equipment was funded by the Knut and Alice Wallenberg Foundation.

Author Contributions: A.E., X.P., S.S. initiated the study, X.P., A.E., R.S. proposed the concept, X.P., A.E., O.O., designed and conducted the experiment, X.P., O.O. processed the data and analyzed the results, O.O. carried out the interpretation and graphical representation of the results, R.S., G.J., S.S., S.P. guided the studies, X.P., O.O., A.E. wrote the manuscript. R.S., G.J., S.S., S.P. edited the manuscript. All authors reviewed the manuscript.

Conflicts of Interest: The authors declare no conflict of interest.

Abbreviations

The following abbreviations are used in this manuscript:

BPS	Blind Phase Search
CD	Chromatic Dispersion
CPR	Carrier Phase Recovery
DAC	Digital to Analog Converter
DDPLL	Decision-Directed Phase-lock-loop
DFRA	Distributed Raman Fiber Amplifier
DSO	Digital Storage Oscilloscope
DSP	Digital Signal Processing
ECL	External Cavity Laser
EDFA	Erbium Doped Fiber Amplifier
HD-FEC	Hard-Decision Forward Error Correction
IQ	In-phase and Quadrature-phase
LO	Local Oscillator
OBPF	Optical Bandpass Filter
PolMux	Polarization Multiplexing
PPG	Pulse Pattern Generator
PSD	Power Spectrum Density
RIN	Relative Intensity Noise
RPN	Relative Phase Noise
SSMF	Standard Single Mode Fiber
QPSK	Quadrature Phase Shift Keying
QPSKP	QPSK Partitioning
QAM	Quadrature Amplitude Modulation
VOA	Variable Optical Attenuator
WDM	Wavelength Division Multiplexer

References

1. Mori, Y.; Zhang, C.; Igarashi, K.; Katoh, K.; Kikuchi, K. Unrepeated 200-km transmission of 40-Gbit/s 16-QAM signals using digital coherent receiver. *Opt. Express* **2009**, *17*, 1435–1441. [CrossRef] [PubMed]
2. Chang, D.; Pelouch, W.; McLaughlin, J. 8 × 120 Gb/s unrepeatered transmission over 444 km (76.6 dB) using Distributed Raman Amplification and ROPA without Discrete Amplification. In Proceedings of the European Conference and Exhibition on Optical Communications (ECOC), Geneva, Switzerland, 19–21 September 2011.
3. Oda, S.; Tanimura, T.; Cao, Y.; Hoshida, T.; Akiyama, Y.; Nakashima, H.; Ohshima, C.; Sone, K.; Aoki, Y.; Yan, M.; et al. 80 × 224 Gb/s Unrepeated Transmission over 240 km of Large-A_{eff} Pure Silica Core Fibre without Remote Optical Pre-amplifier. In Proceedings of the European Conference and Exhibition on Optical Communications (ECOC), Geneva, Switzerland, 19–21 September 2011.
4. Meloni, G.; Potì, L.; Di Nezza, E.; Cavaliere, F.; D'Errico, A.; Magri, R.; Ricci, G. Unrepeated Link Distance Increase for 448 Gb/s Channel Transmission by using Large Core Area. In Proceedings of the European Conference and Exhibition on Optical Communications (ECOC), Geneva, Switzerland, 19–21 September 2011.
5. Downie, J.D.; Hurley, J.; Roudas, I.; Pikula, D.; Garza-Alanis, J.A. Unrepeatered 256 Gb/s PM-16QAM transmission over up to 304 km with simple system configurations. *Opt. Express* **2014**, *22*, 10256–10261. [CrossRef] [PubMed]
6. Rosa, P.; Ania-Castañón, J.-D.; Harper, P. Unrepeatered DPSK transmission over 360 km SMF-28 fibre using URFL based amplification. *Opt. Express* **2014**, *22*, 9687–9692. [CrossRef] [PubMed]
7. Galdino, L.; Tan, M.; Lavery, D.; Rosa, P.; Maher, R.; Phillips, I.D.; Castañón, J.D.A.; Harper, P.; Killey, R.I.; Thomsen, B.C.; et al. Unrepeatered Nyquist PDM-16QAM transmission over 364 km using Raman amplification and multi-channel digital back-propagation. *Opt. Lett.* **2015**, *40*, 3025–3028. [CrossRef] [PubMed]
8. Fludger, C.R.S.; Handerek, V.; Mears, R.J. Pump to Signal RIN Transfer in Raman Fiber Amplifiers. *J. Lightwave Technol.* **2001**, *19*, 1140–1148. [CrossRef]
9. Krause, M.; Cierullies, S.; Renner, H.; Brinkmeyer, E. Pump-to-Stokes RIN transfer in Raman fiber lasers and its impact on the performance of co-pumped Raman amplifiers. *Opt. Commun.* **2006**, *260*, 656–661. [CrossRef]
10. Martinelli, C.; Lorcy, L.; Durecu-Legrand, A.; Mongardien, D.; Borne, S.; Bayart, D. RIN transfer in co-pumped Raman amplifiers using polarization-combined diodes. *IEEE Photonics Technol. Lett.* **2005**, *17*, 1836–1838. [CrossRef]
11. Popov, S.; Vanin, E.; Jacobsen, G. Polarization dependence of gain in discrete Raman amplifiers with dispersion compensating fibres. *J. Opt. A Pure Appl. Opt.* **2002**, *4*, 46–51. [CrossRef]
12. Popov, S.; Sergeyev, S.; Friberg, A.T. The impact of pump polarization on the polarization dependence of the Raman gain due to the breaking of a fibre's circular symmetry. *J. Opt. A Pure Appl. Opt.* **2004**, *6*, S72–S76. [CrossRef]
13. Sergeyev, S.; Popov, S.; Friberg, A.T. Spun fiber Raman amplifiers with reduced polarization impairments. *Opt. Express* **2008**, *16*, 14380–14389. [CrossRef] [PubMed]
14. Sergeyev, S.; Popov, S. Two-section fiber optic Raman polarizer. *IEEE J. Quantum Electron.* **2012**, *48*, 56–60. [CrossRef]
15. Popov, S.; Vanin, E. Polarization dependence of Raman gain on propagation direction of pump and probe signal in optical fibers. In Proceedings of the Lasers and Electro-Optics (CLEO), Baltimore, MD, USA, 6–11 May 2001.
16. Cheng, J.; Tang, M.; Fu, S.; Shum, P.P.; Liu, D. Relative phase noise induced impairment in M-ary phase-shift-keying coherent optical communication system using distributed fiber Raman amplifier. *Opt. Lett.* **2013**, *38*, 1055–1057. [CrossRef] [PubMed]
17. Cheng, J.; Tang, M.; Fu, S.; Shum, P.P.; Liu, D.; Xiang, M.; Feng, Z.; Yu, D. Relative phase noise estimation and mitigation in Raman amplified coherent optical communication system. *Opt. Express* **2014**, *22*, 1257–1266. [CrossRef] [PubMed]
18. Cheng, J.; Tang, M.; Fu, S.; Shum, P.P.; Yu, D.; Wang, L.; Liu, D. Relative Phase noise-Induced Phase Error and System Impairment in Pump Depletion/Nondepletion Regime. *J. Lightwave Technol.* **2014**, *32*, 2277–2286.

19. Cheng, J.; Tang, M.; Lau, A.P.T.; Lu, C.; Wang, L.; Dong, Z.; Bilal, S.M.; Fu, S.; Shum, P.P.; Liu, D. Pump RIN-induced impairments in unrepeatered transmission systems using distributed Raman amplifier. *Opt. Express* **2015**, *23*, 11838–11854. [CrossRef] [PubMed]
20. Xu, L.; Cheng, J.; Tang, M.; Wu, J.; Fu, S.; Shum, P.P.; Liu, D. Experimental Verification of Relative Phase Noise in Raman Amplified Coherent Optical Communication System. *J. Lightwave Technol.* **2016**, *34*, 3711–3716.
21. Tan, M.; Rosa, P.; Le, S.-L.; Phillips, I.-D.; Harper, P. Evaluation of 100G DP-QPSK long-haul transmission performance using second order co-pumped Raman laser based amplification. *Opt. Express* **2015**, *23*, 22181–22189. [CrossRef] [PubMed]
22. Pang, X.; El-Taher, A.; Schatz, R.; Popov, S.; Jacobsen, G.; Sergeyev, S. Characterization of Distributed Raman Amplification-induced Amplitude and Phase Impairments on Unrepeated Coherent Transmission Links. In Proceedings of the Asia Communications and Photonics Conference (ACP), Shanghai, China, 11–14 November 2014.
23. El-Taher, A.; Pang, X.; Schatz, R.; Popov, S.; Jacobsen, G.; Sergeyev, S. Noise Characterization and Transmission Evaluation of Unrepeated Raman Amplified DP-16QAM Link. In Proceedings of the Optical Fiber Communication Conference and Exhibition (OFC), Anaheim, CA, USA, 17–21 March 2013.
24. Borkowski, R.; Zibar, D.; Tafur Monroy, I. Anatomy of a Digital Coherent Receiver. *IEICE Trans. Commun.* **2014**, *E97-B*, 1528–1536. [CrossRef]
25. Zhong, K.; Ke, J.H.; Geo, Y.; Cartledge, J.C. Linewidth-Tolerant and Low-Complexity Two-Stage Carrier Phase Estimation Based on Modified QPSK Partitioning for Dual-Polarization 16-QAM Systems. *J. Lightwave. Technol.* **2013**, *31*, 50–57. [CrossRef]
26. Pfau, T.; Hoffman, S.; Noé, R. Hardware-Efficient coherent digital receiver concept with feed forward carrier recovery for m-QAM constellations. *J. Lightwave. Technol.* **2009**, *27*, 989–999. [CrossRef]
27. Rodrigo Navarro, J.; Kakkar, A.; Pang, X.; Iglesias Olmedo, M.; Ozolins, O.; Da Ros, F.; Piels, M.; Schatz, R.; Zibar, D.; Jacobsen, G.; et al. Two-Stage n-PSK Partitioning Carrier Phase Recovery Scheme for Circular mQAM Coherent Optical Systems. *Photonics* **2016**, *3*, 37. [CrossRef]
28. Kikuchi, K. Characterization of semiconductor-laser phase noise and estimation of bit-error rate performance with low-speed offline digital coherent receivers. *Opt. Express* **2012**, *20*, 5291–5302. [CrossRef] [PubMed]